

Article

Hydrophobic Calcium Carbonate for Cement Surface

Shashi B. Atla ¹, Yi-Hsun Huang ², James Yang ¹, How-Ji Chen ^{2,†,*}, Yi-Hao Kuo ²,
Chun-Mei Hsu ³, Wen-Chien Lee ³, Chien-Cheng Chen ⁴, Duen-Wei Hsu ⁴
and Chien-Yen Chen ^{1,†,*} 

¹ Department of Earth and Environmental Sciences, National Chung Cheng University, 168 University Road, Minhsiung, Chiayi County 62102, Taiwan; shashi_org@yahoo.com (S.B.A.); chieyechen@yahoo.com (J.Y.)

² Department of Civil Engineering, National Chung Hsing University, 250 Kuo Kuang Road, Taichung 4022, Taiwan; x699237014x@gmail.com (Y.-H.H.); yhkao31@gmail.com (Y.-H.K.)

³ Department of Chemical Engineering, National Chung Cheng University, 168 University Road, Ming-Shung, Chiayi County 62102, Taiwan; gupi_girl@livemail.tw (C.-M.H.); chmwcl@ccu.edu.tw (W.-C.L.)

⁴ Department of Biotechnology, National Kaohsiung Normal University, No.62 Shenjhong Road, Yanchao Township, Kaohsiung County 82444, Taiwan; cheng@nknknu.edu.tw (C.-C.C.); duenwei.hsu@gmail.com (D.-W.H.)

* Correspondence: hojichen@nchu.edu.tw (H.-J.C.); chien-yen.chen@oriel.oxon.org (C.-Y.C.); Tel.: +886-5-2720411 (ext. 66220) (C.-Y.C.)

† These authors contributed equally to this work.

Academic Editor: Linda Pastero

Received: 14 November 2017; Accepted: 8 December 2017; Published: 11 December 2017

Abstract: This report describes a novel way to generate a highly effective hydrophobic cement surface via a carbonation route using sodium stearate. Carbonation reaction was carried out at different temperatures to investigate the hydrophobicity and morphology of the calcium carbonate formed with this process. With increasing temperatures, the particles changed from irregular shapes to more uniform rod-like structures and then aggregated to form a plate-like formation. The contact angle against water was found to increase with increasing temperature; after 90 °C there was no further increase. The maximum contact angle of 129° was obtained at the temperature of 60 °C. It was also found that carbonation increased the micro hardness of the cement material. The micro hardness was found to be dependent on the morphology of the CaCO₃ particles. The rod like structures which caused increased mineral filler produced a material with enhanced strength. The ¹³C cross polarization magic-angle spinning NMR spectra gave plausible explanation of the interaction of organic-inorganic moieties.

Keywords: SEM; X-ray diffraction; carbonation; micromechanics; CaCO₃; cement

1. Introduction

Synthesis of organic-inorganic hybrids has received a great deal of attention in the field of material science [1] because it can result in the creation of multifunctional materials. The applications of hybrid organic-inorganic materials are found in various fields such as optics, electronics, energy, housing and the environment [2]. The desired function can be delivered from manipulating organic or inorganic or both components.

It is fair to say that modern civilizations have depended to a large degree on concrete material for the history of concrete usage, please see [3]. Various properties of concrete can be fabricated for specific applications. Concrete, however, is potentially vulnerable to a variety of different exposures unless some certain precautions are taken. Durability of concrete has serious economic implications in the form of maintenance and replacement costs of a structure. Therefore, in designing structures, the durability characteristics of the concrete should be evaluated as carefully as other aspects such

as mechanical properties, hardness, and initial coast. Permeability is a determinant parameter that has the largest influence on the durability of concrete; the size and continuity of the pores in hydrated cement mortar would control the coefficient of permeability [4]. To decrease the permeability of concrete, the waterproofing treatment is recognized as an effective way. For waterproofing treatments, it requires the impregnation of concrete walls with hydrophobic agents. Hydrophobic treatment prevents wetting of the concrete's porous structure. A great number of organic additives have been studied as hydrophobic reagents including alkyl-alkoxy silane [5,6], surfactants [7,8], acrylic and polyurethane [6,9]. Concrete carbonation is a process in which carbondioxide reacts with calcium hydroxide [10–12] in the cement matrix to form calcium carbonate and water and the reaction stoichiometry is: $\text{Ca(OH)}_2 + \text{CO}_2 \rightarrow \text{CaCO}_3 + \text{H}_2\text{O}$.

There are many reports on the synthesis of hydrophobic calcium carbonate via carbonation route [13]. Hydrophobic calcium carbonate leads to many industrial applications. It is used as pigment, mortar, and abrasive and in paper and plastic as a filler [14]. Chen et al. have reported carbonation of Ca(OH)_2 to synthesize cubic CaCO_3 using dodecanoic acid as modifier [13]. Several organic additives used for synthesizing hydrophobic CaCO_3 via carbonation of Ca(OH)_2 include oleic acid [15], octadecyl dihydrogen phosphate [16], sodium oleate [17], stearic acid [18], and dodecanoic acid [19]. Various hydrophobic admixtures have been examined for concrete and mortar. In many cases the admixture caused damage, e.g., greater decay of samples in the frost resistance test. Some admixtures are effective, but their selection must be confirmed by further research [20,21].

No study, however, has yet been reported on synthesis of hydrophobic cement surface material via carbonation route. For many years, metal soaps have been studied for the hydrophobic properties, but have not been used in hydrophobising building materials in practice [12]. This is because the by-products of the use of soaps are water-soluble salts that lead to increased hygroscopicity of the material [22]. In addition, it is not recommended to use soaps for the hydrophobising of building surfaces due to its low resistance to dirt, mechanical damage and salinity [23,24]. Another unfavorable factor includes interference with the cement hydration process in the presence of a hydrophobic compound that decreases the compressive strength of materials. Currently, only the organosilicon compounds are used for hydrophobisation concrete with Portland cement. However, the disadvantage of this hydrophobic cement is that it is very expensive [21,25,26].

In this report we describe a feasible single step involving in situ synthesis of hydrophobic cement surface with stearic acid. We found that the temperature of carbonation reaction has a great deal of effect on morphology of CaCO_3 and thus the hydrophobicity of the concrete surface. Furthermore, the carbonation and mineralization improved the surface micro hardness of the samples.

2. Experimental Section

Type I Portland cement based on ASTM C150 and Ottawa sand with the size distribution from 0.1 mm to 1 mm were used. A cement mortar was made from Portland cement with saturated surface dry sand, and tap water in the ratio of 4:11:2, and was cast into 2.5 cm cubes in an acrylic mold. The cubes were conserved at room temperature for a day and curing was done by continuous immersion in supersaturated solution of Ca(OH)_2 for one week. The cement blocks were then taken for carbonation reaction. Carbonation reaction was done in an autoclave (Autoclave Engineers, $V = 500 \text{ cm}^3$) at CO_2 pressure of 2 kgf/cm^2 . The organic solution was prepared by taking 1:1 molar ratio (0.004 moles) of stearic acid and sodium hydroxide in 400 mL of deionized water. The mixture was stirred at 70°C for 5 min and was filled so as to cover cubes in the autoclave. The autoclave was sealed and pressurized with CO_2 to a desired pressure. The carbonation reaction was carried out at different temperatures (30, 60, 90, 120 and 150°C) for a period of 24 h. After this, the reactor was allowed to attain room temperature and CO_2 gas was vented off, and the cubes were oven dried at 50°C for one day. The cement cubes without organic solution and carbonation are referred to as “control experiments”. The cement cubes with organic solution and without carbonation are referred to as “Ctrl-2 experiments”.

A small quantity of the material was scrapped from the cube surface and was characterized by XRD, IR and SEM. Powder X-ray diffraction (XRD) patterns were recorded on a Shimadzu X-ray diffractometer (LabX XRD-6000, Shimadzu, Tokyo, Japan) equipped with Ni-filtered $\text{CuK}\alpha$ ($\lambda = 0.1541$ nm, 4 kVA, 30 mA) radiation and a graphite crystal monochromator. SEM measurements were carried out on a Leica Stereoscan-440 scanning electron microscope (SEM, Leica, Cambridge, UK) equipped with a Phoenix EDAX attachment (Mahwah, NJ, USA). The water contact angles of the samples were measured using FTA 2000 contact angle goniometer (First Ten Angstroms, Portsmouth, VA, USA) by the sessile drop method using a micro syringe at 25 °C. FTIR spectra of the samples were recorded on a Shimadzu 8300 FTIR spectrometer (Shimadzu, Tokyo, Japan). Microhardness was measured using a micro-indentation tester (Shimadzu Micro Hardness Testers HMV-2, Shimadzu Corporation, Kyoto, Japan). The spectra of solid state NMR were performed using Bruker Avance III 400 NMR Spectrometer (Bruker, Billerica, MA, USA).

3. Results and Discussion

Figure 1 shows the XRD spectrum of the control and the carbonated cement cubes at different temperatures. The major peak of the controlled experiment were comprised of crystalline SiO_2 diffraction signal value at $2\theta = 26.66^\circ$. It is well known that SiO_2 is the common major constituent of the sand. On the other hand, XRD of the carbonated samples showed formation of a new peak at $2\theta = 29.32^\circ$, which corresponds to that of calcite peak (CaCO_3). Among the polymorphs of CaCO_3 (calcite, aragonite, and vaterite), calcite is the thermodynamically stable phase under ambient conditions. This clearly indicates that carbonation has taken place in the materials undertaken for this study. Solid state ^{13}C CP-MAS NMR also corroborates this and is discussed in the later section. Besides the peaks of SiO_2 and CaCO_3 , few peaks at higher carbonation temperatures (60 and 90 °C) arise, which may be attributed to the association of organic molecule with the cement matrix to form calcium stearate. Ozturk et al. have reported the synthesis and X-ray diffraction of calcium stearate [27]. As per the synthesis procedure we synthesized 50% excess calcium stearate precipitate and obtained XRD spectrum which showed a high intensity diffraction peak at 2θ value of 19.96° . We assume small peaks near 20° to be associated with calcium stearate in the cement matrix. Several typical vibrations bands of pure stearate molecules, including 2920, 2848 and 1463 cm^{-1} in the FTIR spectrum of stearate with different temperatures, are also observed (Figure S1).

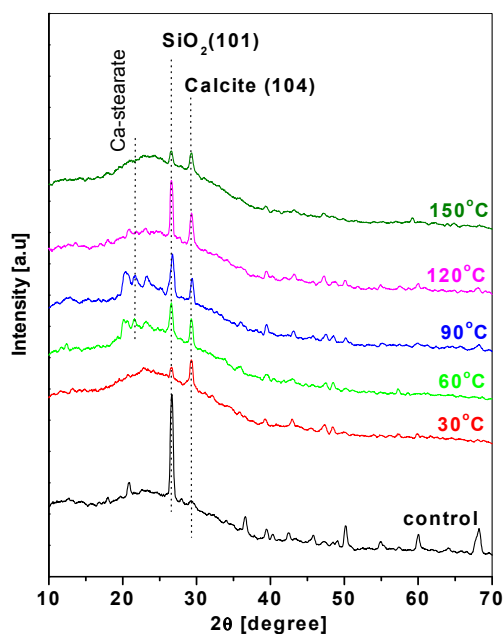


Figure 1. XRD pattern obtained from controlled and carbonated samples at different temperatures.

Figure 2 shows the SEM images of the carbonated samples, which showed differences in particle morphology that were strongly dependent on carbonation reaction temperature. At 30 °C, the product has irregular morphology (flat surfaces). At temperatures of 60 and 90 °C, these irregular particles transformed to form rod like structures and at higher temperatures of 120 and 150 °C the rod like structures transformed to aggregate particles (plate-like). The series of interactions between $\text{Ca}(\text{OH})_2$ in the cement matrix, stearic acid and CO_2 varied with increasing carbonation reaction temperatures which gave rise to products with different morphology.

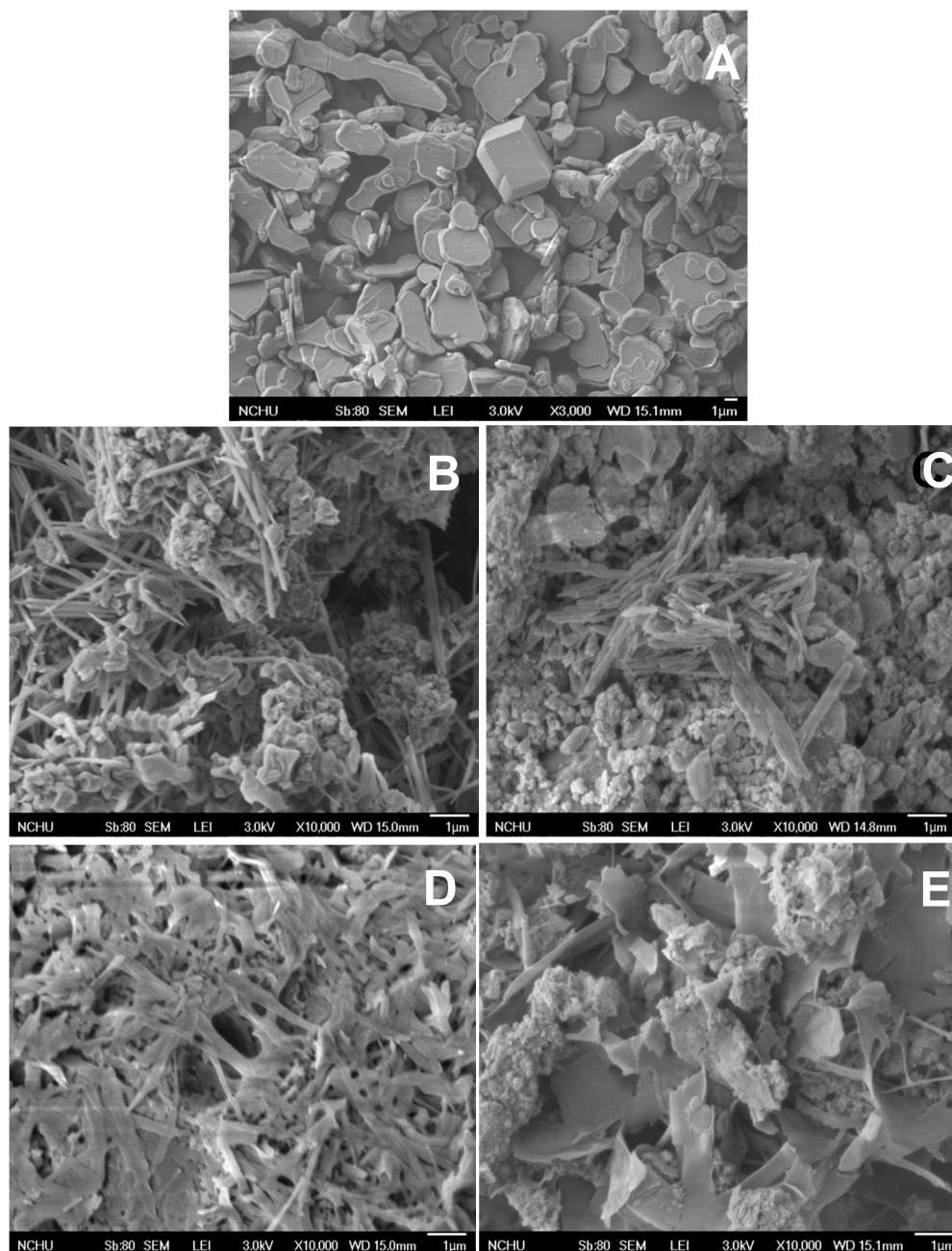


Figure 2. SEM images of the carbonated samples (A) 30 °C, (B) 60 °C, (C) 90 °C, (D) 120 °C, (E) 150 °C.

The FTIR spectra of the carbonated samples showed (Figure 3) the characteristic peaks of calcium stearate. The interaction of Ca^{2+} and organic substrate with COO^- functionality is already known in the literature [15]. Calcium stearate can be formed by the reaction of the COO^- of the stearic acid and Ca^{2+} ions to form a cover on the surface of CaCO_3 particles. The peaks at 1577 and 1541 cm^{-1}

are due to antisymmetric stretching bands for unidentate and bidentate association with calcium ions. The antisymmetric and symmetric methylene stretching were observed at 2916 and 2849 cm^{-1} respectively. These results are in agreement with functional groups present for calcium stearate [27]. The IR results showed that the intensity of CH_2 stretching band increased initially for the temperatures from 30 to 90 $^{\circ}\text{C}$ and then decreased with further increase in temperature. This suggests that the surface modification of CaCO_3 is reduced at higher temperatures.

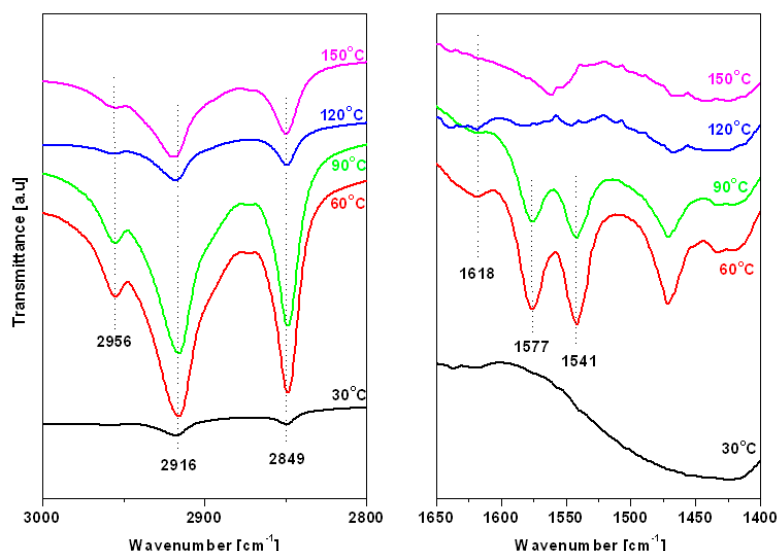


Figure 3. FTIR spectra of the carbonated samples at different temperatures.

In order to further investigate the structure elucidation of the synthesized samples, solid-state NMR spectroscopy was utilized in this study. Figure 4 presents the schematic of organic-inorganic interaction on the surface of the cement matrix. The Ca^{2+} reacts with $\text{CH}_3(\text{CH}_2)_{16}\text{COO}^-$ to form hydrophobic $\text{Ca}(\text{CH}_3(\text{CH}_2)_{16}\text{COO})_2$, and thus formed $\text{Ca}(\text{CH}_3(\text{CH}_2)_{16}\text{COO})_2$ are deposited on the CaCO_3 precipitate formed during the carbonation of $\text{Ca}(\text{OH})_2$.

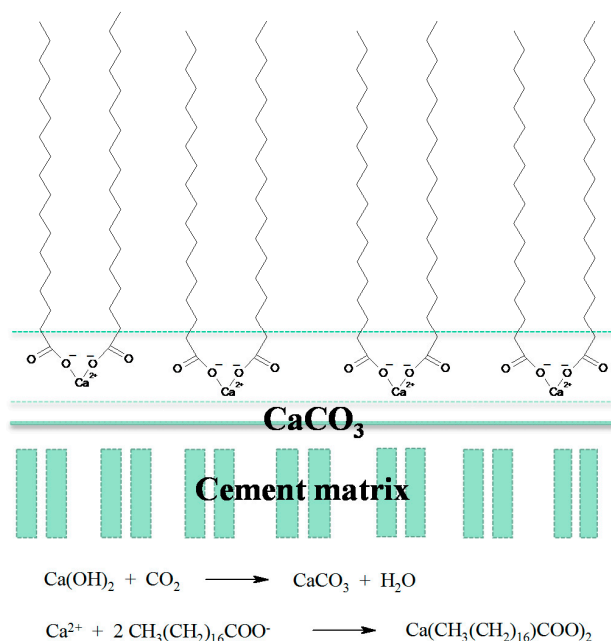


Figure 4. Schematic of the stearate molecules on CaCO_3 in cement matrix.

For NMR, samples obtained at 90 °C carbonation were used as a material for case study. Calcium stearate (50% excess Ca) were taken as reference material for comparing with the carbonated cement material. The solid state ^{13}C NMR spectras are presented in Figure 5. Figure 5a shows the NMR spectrum of pure calcium stearate. The carbonyl carbon (C1) signal exhibits at a resonance frequency of about 185.4 ppm (normal stearic acid C1 position is at 179 ppm [28]). The methyl (CH_3) and methylene (CH_2) group of calcium stearate resonates in the frequency range of 14.6–39.9 ppm. The high intensity peak at 33.05 ppm is due to CH_2 group (C4–C16) indicating their higher population of alkyl chain in the calcium stearate structure. The C1, C2, C3, C17, and C18 peaks are difficult to detect in the spectrum of cement block materials as compared to pure calcium stearate. Figure 5b shows the carbonation of cement block without any sodium stearate, the formation of ^{13}C peak arises due to the formation of CaCO_3 and its chemical shift value is 169.12. This data clearly indicates that carbonation has taken place in our samples. Figure 5c shows the carbonation in the presence of sodium stearate. The presence of signal at chemical shift value of 33.5 ppm can be attributed to the presence of stearate molecules, and the peak signal at 168.6 ppm arises from CaCO_3 . There is slight change in peak value of CH_2 group (C4–C16) after surface modification (33.5 ppm) as compared to pure calcium stearate (33.05 ppm). There is also a change in peak value of the corresponding ^{13}C peak of CaCO_3 in the presence (168.6) of stearate molecules (absence 169.12). This upfield shift of CaCO_3 arises due to shielding effect and clearly indicates surface modifications of cement blocks in the presence of stearate molecule. These studies also suggest plausible explanation of the organic-inorganic moieties interaction as shown in Figure 4.

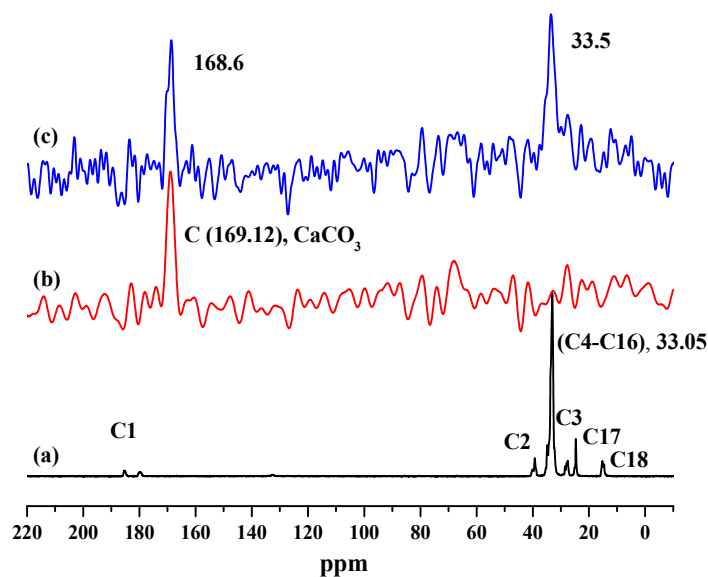


Figure 5. Solid-state ^{13}C CP-MAS NMR (a) calcium stearate (b) carbonation of cement without stearate (c) carbonation in the presence of stearate.

The hydrophobic function is often demonstrated with water contact angle and is sometimes referred to as “lotus effect”. Hydrophobicity is controlled both by hydrophobic substrate film and the roughness of the surface. To show the lotus effect, hydrophobicity as the basis for self-cleaning mechanism, the organic interaction characteristic of cement surface was measured by contact angle. The organic additive changes the property of concrete material in situ, Figures 6 and 7a show the contact angle of the cement surfaces obtained at different carbonation reaction temperatures. At lower reaction temperature (30 °C), the contact angle against the hydrophobized cement surface was zero. The contact angle increased to 129 and 125° respectively for the temperatures 60 and 90 °C. Temperature increases the efficient interaction of stearate molecules and Ca^{2+} and CO_3^{2-} inducing hydrophobic calcite hence an increment in the contact angle. However, further increase in temperature caused

a slight decrease in the contact angle and remained constant after 90 °C. The surface roughness also seems to play an important role in enhancing or decreasing the hydrophobicity [29]. The results of IR and contact angle are in accordance with each other. On the other hand, contact angle of Ctrl-2 experiment at 90 °C was found to be ~80° (other samples were not studied); this indicates that CO₂ plays an important role in enhancing the hydrophobicity of the cement surface.

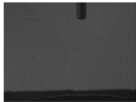
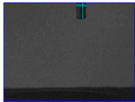
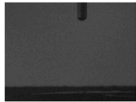
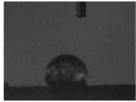
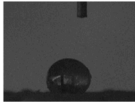
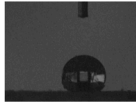
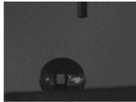
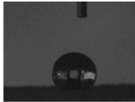
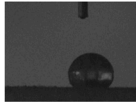
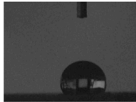
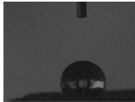
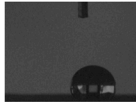
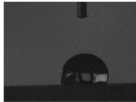
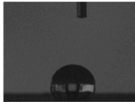
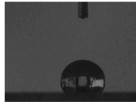
sample	1 st	2 nd	3 rd	average water contact angle
30°C				0°
60°C				129°
90°C				124.67°
120°C				114.83°
150°C				115.5°

Figure 6. Water contact angle study on cement surfaces prepared by carbonation at different temperatures.

Micro structural features in cement systems such as porosity, pore structure, density, crystallinity and morphology, may affect the dependence of the fracture terms on microhardness. In our experiments, the micro hardness value first increases and then decreases with temperature as shown in Figure 7a. From SEM images, the rod like structures of CaCO₃ at 60 and 90 °C caused increased calcite fiber mineral filler that bridged between cement particles, and thus they enhanced micro hardness of the interface. Microhardness of the carbonated samples was compared with that of the Ctrl-2 experiments as shown in Figure 7b. The carbonated samples showed higher microhardness of the cement surface, which was found to be dependent on the morphology of the carbonated samples.

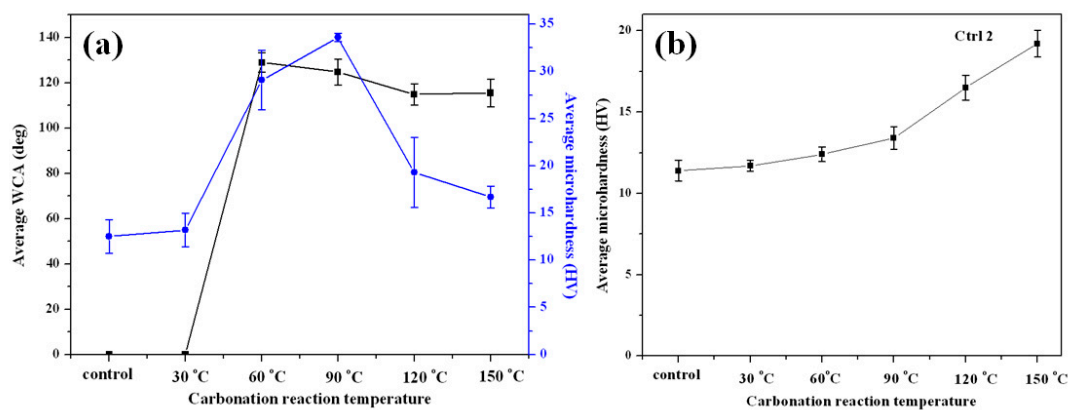


Figure 7. (a) Double Y axis graph showing contact angle of the cement surface against water and micro hardness of cement blocks obtained at different carbonation reaction temperature; (b) microhardness of cement cubes of Ctrl 2 experiments.

4. Conclusions

We have succeeded in obtaining hydrophobic cement surface via carbonation with the surface treatment with stearic acid in situ. The alkyl chain of stearic acid makes the CaCO_3 hydrophobic. Our study showed that at carbonation temperatures of 60 and 90 °C, maximum surface treatment with the stearic acid takes place as was seen from both the IR and contact angle. The different reaction temperature produced different morphology of the CaCO_3 particles, and the rod like structures enhanced the microhardness of the samples. NMR studies also suggest the presence of organic-inorganic interactions. The synthesis of the hydrophobicity does not guarantee the effectiveness of the use of cement in concrete and construction. This is because the cement grains are surrounded by a hydrophobic coating, which makes it difficult or impossible to hydrate the cement. Hence, this leads to the decrease in compressive strength and the loss of sample mass after freezing-thawing [6]. Admixture hydrophobic creates chemical bonds between the individual components of concrete, affecting the changes in the microstructure, as well as changing the strength parameters [30]. The carbonation of cement surface seems to be a promising route to synthesize hydrophobic surface and its properties can be tailored by using different organic additives.

Supplementary Materials: The following are available online at www.mdpi.com/2073-4352/7/12/371/s1, Figure S1: FTIR spectrum of pure stearate stored at different temperatures.

Acknowledgments: The authors are very grateful to the Ministry of Science and Technology in Taiwan for sponsoring this research.

Author Contributions: James Yang, Yi-Hsun Huang and Chun-Mei Hsu conceived and designed the experiments; Yi-Hao Kuo and How-Ji Chen performed the experiments; Duen-Wei Hsu and Shashi B. Atla analyzed the data; Wen-Chien Lee contributed reagents/materials/analysis tools; Shashi B. Atla, Chien-Yen Chen and Chien-Cheng Chen wrote the paper.

Conflicts of Interest: The authors declare no conflict of interest.

References

1. Naka, K.; Chujo, Y. Control of Crystal Nucleation and Growth of Calcium Carbonate by Synthetic Substrates. *Chem. Mater.* **2001**, *13*, 3245–3259. [[CrossRef](#)]
2. Sanchez, C.; Belleville, P.; Popall, M.; Nicole, L. Applications of advanced hybrid organic-inorganic nanomaterials: From laboratory to market. *Chem. Soc. Rev.* **2011**, *40*, 696–753. [[CrossRef](#)] [[PubMed](#)]
3. Mindess, S.; Young, J.F.; Darwin, D. *Concrete*; Prentice Hall: Upper Saddle River, NJ, USA, 2003.
4. Monteiro, P.J.M.; Mehta, P.K. *Concrete: Structure, Properties, and Materials*; Prentice-Hall, Inc.: Upper Saddle River, NJ, USA, 1986.
5. Basheer, P.A.M.; Basheer, L.; Cleland, D.J.; Long, A.E. Surface treatments for concrete: Assessment methods and reported performance. *Constr. Build. Mater.* **1997**, *11*, 413–429. [[CrossRef](#)]
6. Tkach, E.V.; Semenov, V.S.; Tkach, S.A.; Rozovskaya, T.A. Highly Effective Water-repellent Concrete with Improved Physical and Technical Properties. *Procedia Eng.* **2015**, *111*, 763–769. [[CrossRef](#)]
7. Zhang, T.; Shang, S.; Yin, F.; Aishah, A.; Salmiah, A.; Ooi, T.L. Adsorptive behavior of surfactants on surface of Portland cement. *Cem. Concr. Res.* **2001**, *31*, 1009–1015. [[CrossRef](#)]
8. Maryoto, A. Resistance of Concrete with Calcium Stearate Due to Chloride Attack Tested by Accelerated Corrosion. *Procedia Eng.* **2017**, *171*, 511–516. [[CrossRef](#)]
9. Medeiros, M.H.F.; Helene, P. Surface treatment of reinforced concrete in marine environment: Influence on chloride diffusion coefficient and capillary water absorption. *Constr. Build. Mater.* **2009**, *23*, 1476–1484. [[CrossRef](#)]
10. Park, D.C. Carbonation of concrete in relation to CO_2 permeability and degradation of coatings. *Constr. Build. Mater.* **2008**, *22*, 2260–2268. [[CrossRef](#)]
11. Izaguirre, A.; Lanas, J.; Álvarez, J.I. Effect of water-repellent admixtures on the behaviour of aerial lime-based mortars. *Cem. Concr. Res.* **2009**, *39*, 1095–1104. [[CrossRef](#)]
12. Maryoto, A. Improving Microstructures of Concrete Using $\text{Ca}(\text{C}_{18}\text{H}_{35}\text{O}_2)_2$. *Procedia Eng.* **2015**, *125*, 631–637. [[CrossRef](#)]

13. Chen, Y.; Ji, X.; Zhao, G.; Wang, X. Facile preparation of cubic calcium carbonate nanoparticles with hydrophobic properties via a carbonation route. *Powder Technol.* **2010**, *200*, 144–148. [[CrossRef](#)]
14. Keum, D.-K.; Kim, K.-M.; Naka, K.; Chujo, Y. Preparation of hydrophobic CaCO_3 composite particles by mineralization with sodium trisilanolate in a methanol solution. *J. Mater. Chem.* **2002**, *12*, 2449–2452. [[CrossRef](#)]
15. Wang, C.; Sheng, Y.; Hari, B.; Zhao, X.; Zhao, J.; Ma, X.; Wang, Z. A novel aqueous-phase route to synthesize hydrophobic CaCO_3 particles in situ. *Mater. Sci. Eng. C* **2007**, *27*, 42–45. [[CrossRef](#)]
16. Wang, C.; Xiao, P.; Zhao, J.; Zhao, X.; Liu, Y.; Wang, Z. Biomimetic synthesis of hydrophobic calcium carbonate nanoparticles via a carbonation route. *Powder Technol.* **2006**, *170*, 31–35. [[CrossRef](#)]
17. Sheng, Y.; Zhou, B.; Wang, C.; Zhao, X.; Deng, Y.; Wang, Z. In situ preparation of hydrophobic CaCO_3 in the presence of sodium oleate. *Appl. Surf. Sci.* **2006**, *253*, 1983–1987. [[CrossRef](#)]
18. Wang, C.; Sheng, Y.; Zhao, X.; Pan, Y.; Hari, B.; Wang, Z. Synthesis of hydrophobic CaCO_3 nanoparticles. *Mater. Lett.* **2006**, *60*, 854–857. [[CrossRef](#)]
19. Wang, C.; Piao, C.; Zhai, X.; Hickman, F.N.; Li, J. Synthesis and characterization of hydrophobic calcium carbonate particles via a dodecanoic acid inducing process. *Powder Technol.* **2010**, *198*, 131–134. [[CrossRef](#)]
20. Jumate, E.; Manea, D.L.; Moldovan, D.; Fechet, R. The Effects of Hydrophobic Redispersible Powder Polymer in Portland Cement Based Mortars. *Procedia Eng.* **2017**, *181*, 316–323. [[CrossRef](#)]
21. Falchi, L.; Zendri, E.; Müller, U.; Fontana, P. The influence of water-repellent admixtures on the behaviour and the effectiveness of Portland limestone cement mortars. *Cem. Concr. Compos.* **2015**, *59*, 107–118. [[CrossRef](#)]
22. Izaguirre, A.; Lanás, J.; Álvarez, J.I. Ageing of lime mortars with admixtures: Durability and strength assessment. *Cem. Concr. Res.* **2010**, *40*, 1081–1095. [[CrossRef](#)]
23. Maranhão, F.; John, V.; Loh, K.; Pileggi, R. The influence of silicone based water repellents as admixtures on the rheological properties of cement slurry. In Proceedings of the Hydrophobe V, 5th International Conference on Water Repellent Treatment of Building Materials, Brussels, Belgium, 15–16 April 2008; pp. 255–258.
24. Klisińska-Kopacz, A.; Tišlova, R. Effect of hydrophobization treatment on the hydration of repair Roman cement mortars. *Constr. Build. Mater.* **2012**, *35*, 735–740. [[CrossRef](#)]
25. Falchi, L.; Müller, U.; Fontana, P.; Izzo, F.C.; Zendri, E. Influence and effectiveness of water-repellent admixtures on pozzolana–lime mortars for restoration application. *Constr. Build. Mater.* **2013**, *49*, 272–280. [[CrossRef](#)]
26. Xue, X.; Li, Y.; Yang, Z.; He, Z.; Dai, J.-G.; Xu, L.; Zhang, W. A systematic investigation of the waterproofing performance and chloride resistance of a self-developed waterborne silane-based hydrophobic agent for mortar and concrete. *Constr. Build. Mater.* **2017**, *155*, 939–946. [[CrossRef](#)]
27. Gönen, M.; Öztürk, S.; Balköse, D.; Okur, S.; Ülkü, S. Preparation and Characterization of Calcium Stearate Powders and Films Prepared by Precipitation and Langmuir–Blodgett Techniques. *Ind. Eng. Chem. Res.* **2010**, *49*, 1732–1736. [[CrossRef](#)]
28. Cunningham, I.D.; Courtois, J.-P.; Danks, T.N.; Heyes, D.M.; Moreton, D.J.; Taylor, S.E. Synthesis and characterisation of calixarene-stabilised calcium carbonate overbased detergents. *Colloids Surf. A Physicochem. Eng. Asp.* **2003**, *229*, 137–147. [[CrossRef](#)]
29. Bhushan, B.; Jung, Y.C. Natural and biomimetic artificial surfaces for superhydrophobicity, self-cleaning, low adhesion, and drag reduction. *Prog. Mater. Sci.* **2011**, *56*, 1–108. [[CrossRef](#)]
30. Corinaldesi, V. Combined effect of expansive, shrinkage reducing and hydrophobic admixtures for durable self compacting concrete. *Constr. Build. Mater.* **2012**, *36*, 758–764. [[CrossRef](#)]

